Paper No. 100

ISMS 2016

Study on the similar materials simulation of the slope stability of the west-Ⅰ zone in Luming Molybdenum Mine

Huang Zhian, YangFei, Wang Hui*, Zhang Yinghua, GaoYukun

State Key Laboratory of High-Efficient Mining and Safety of Metal Mines (University of Science and Technology Beijing), Ministry of Education, Beijing 100083, China

ABSTRACT
Based on a study of the geological data and rock mechanics parameters of the Luming Molybdenum Mine and according to the slope stability in the excavation process of the weak structure of the mining area, the similar material simulation test was developed. Using the proportion of geometric similarity constant 300, the laboratory model was set up for a 3-3 profile, and arranged with displacement monitoring points and stress monitoring points. Then the excavation process of the actual slope was simulated with this model and finally conclusions were made after collecting relevant data, as follows: in the process of open-pit slope excavation, the bench slope was affected by a weak structural plane and excavation disturbance. The bench slope was destroyed due to deformation failure, especially in the cross area of the weak structure plane and fault and the area of the bench slope located in weak structural plane.
KEYWORDS: slope; stability; similarmaterial; experimental simulation

1. INTRODUCTION

Research on stability for slope engineering has always been one of the core problems in the field of mining engineering, and the main content of slope engineering research relates to the mechanisms of deformation and failure. Under the comprehensive effect of various internal and external factors, stability is characterized by certainty and randomness, making it difficult to adopt the mathematical analytical method to solve the problem of stability for slope engineering (Yang, T.H. et al., 2011). Directly using an experimental study of the actual structure size is also impossible and has great limitations. With the principles of similarity theory, using the similar physical model for slope stability research has been one of the effective ways to solve the problem of slope engineering, and the development of slope engineering research also shows that it is an effective method.

Based on the experiment method of the similar material simulation, this study simulates the Luming Molybdenum west-I area slope engineering deformation and failure process, and studies the deformation and failure rules. The test of similar material mixture is conducted to get all kinds of material proportion, then a similar material simulation experiment is conducted to simulate the excavation sequence, and finally the stress and displacement data are collected for stability analysis (Yin, Z.G. et al., 2011; Zhang, H. et al, 2011). Combined with the numerical simulation results, the purpose of this study is to find the 3-3 section of Luming Molybdenum on the west-I slope potential damage area through a similar material simulation, and to provide technical support for the safety production.

2. THE BASIC PRINCIPLE OF SIMILAR EXPERIMENTS

The theoretical basis of similar material simulation experiment are three laws, according to the theory of similarity, and they are mainly geometric similarity, kinetic similarity, and dynamical similarity which are to satisfy the single value geometric conditions, physical conditions and time conditions, boundary conditions, and initial conditions (Wu, W., 2011). The similarity criteria are as follows:

(1) Geometric similarity

$$\frac{L_m}{L_p} = C_l \quad (1)$$

In the formula: M represents the similar model, P represents the engineering prototype, C is similarity ratio, the same below.

(2) Time similarity

$$C_t = \sqrt{C_l} \quad (2)$$

(3) Bulk density similarity

*Corresponding author – email :wanghuiustb@live.cn.

$$\frac{\gamma_m}{\gamma_p} = C_\gamma \quad (3)$$

(4) Stress similarity (elastic modulus, strength, etc):

$$\frac{\sigma_m}{\sigma_p} = C_\sigma = C_\gamma \cdot C_l \quad (4)$$

$$(C_E = C_\gamma \cdot C_l \ , \ C_R = C_\gamma \cdot C_l \ )$$

3. MODEL SELECTION AND THE SELECTION OF SIMILAR MATERIAL

3.1 Selection of similar model

This study is based on the investigation of geological data and mechanical parameters of rock mechanics parameters in the early period of a mining area, and the area of potential safety hazard is mainly in the fault area of F4 and F3. In order to confirm with numerical simulation research, the profile of the selected analog simulation is 3-3 section (as shown in Figure 1). Rock mechanics parameters are shown in Table 1.

Table 1: Rock and soil physical and mechanical parameter table of west-Ⅰ area slope engineering of Luming Molybdenum.

Lithology	Density	Elasticity modulus	Poisson's ratio	Shear elasticity	Internal friction angle	Cohesive force	Compressive strength	Depth
	103kg/m^3	GPa		GPa	°	MPa	MPa	m
Granite 1	2.526	4.82	0.28	1.88	29	0.12	0.061	0-93
Granite 2	2.592	5.34	0.23	2.17	33	0.21	0.457	93-147
Granite 3	2.614	6.52	0.2	2.72	37	0.25	0.512	147-
Crushed zone	2.173	1.44	0.33	0.54	19.01	0.075	0	

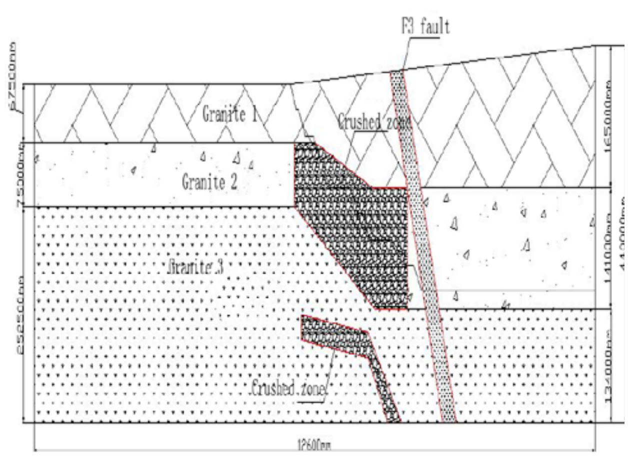

Figure 1: 3-3 Profile geological map.

2.2 Determine similar conditions

(1) The geometric similarity constant

Length similarity constant: $\alpha_L = L_H/L_M$, L_H-the thickness of prototype, L_M-the thickness of model. In the choice of geometric similarity constant α_L=300 (empirical value), due to the fact that the prototype height is 440 m and the horizontal width is 1260 m, the simulation size, height, and thickness should be 4200 m, 1467 m, 250 m, respectively.

The planestrain conditions are used in the experiment, and the thickness of each layer in the similar model are respectively:

$L_{M1} = L_{H1} / a_L$ =50 m/300=167 mm；

In the same way, the thickness of L_{M2}, L_{M3}, L_{M4} are 300 mm, 297 mm, 870 mm.

(2) The time similarity constant

$$a_t = \sqrt{a_L} = (300)^{1/2} = 17.32$$

(3) The bulk density similarity constant

$\alpha_\gamma = \gamma_H / \gamma_M$, γ_H -prototype unit weigh, γ_M -model bulkdensity. γ_M -generally is13.7-17.68 kN/m^3, after considering comprehensively the option is 16.5 kN/m^3.

With the granite 1 unit weight as the prototype unit weight, the unit weight similar constant is calculated as follows:

$$\alpha_\gamma = \gamma_H / \gamma_M = \frac{2.526 \times 9.8}{16.5} = 1.5$$

(4) The intensity of similar constant

$\alpha_C = C_H/C_M$, C_H-the intensity of the prototype, C_M-the model intensity. The intensity similarity constant is equal to the density of similar strength.

(5) Stress similarity constant

$$\alpha_\sigma = \frac{\sigma_H}{\sigma_M} = \frac{\gamma_H H_H}{\gamma_M H_M} = \alpha_L \frac{\gamma_H}{\gamma_M} \quad (5)$$

So, $\alpha_\sigma = \alpha_L \cdot \gamma_H / \gamma_M \approx 450$

Type: σ_H—the original rock stress or strength; the unit is kN/m^3, same below.

σ_M —the stress or strength of model; σ_p—prototype average density

2.3 The selection of similar material, strength calculation and material ratio

River sand was chosen as the raw material, where the density is 1.35-1.45 g/cm^3, lime and gypsum as cement, and the density is 2.60-2.75 g/cm^3 and 0.936 g/cm^3.

The model strength is calculated, according to the similarity calculation formula:

$$\sigma_M = \sigma_p / \alpha_L \alpha_\gamma \quad (6)$$

Type: σ_M- simulation strength of the rock (ore) in the model, unit for MPa; σ_p- actual strength of the rock(ore) in the prototype, unit for MPa.

α_L、α_γ represent the geometric similarity ratio and bulk density, respectively. Therefore, the simulated strength of the corresponding rock is: the compressive strength and bulk density of the first layer of granite model, which are:

$$\sigma_{M1} = 19.37 \times \frac{1}{300 \times 1.5} = 0.043(MPa) \; ;$$

$$\gamma_{M1} = \frac{\gamma_H}{\alpha_\gamma} = \frac{2.526}{1.5} = 1.68 \, \text{kN}/m^3 \; ;$$

In the same way, as for the second and third layer of the granite and the fracture zone model, the compresive strength of σ_{M2}, σ_{M3}, σ_{M4} are 0.102 MPa, 0.114 MPa, 1.78×10^{-4} MPa and the bulk density for γ_{M2}, γ_{M3}, γ_{M4} are 1.728 kN/m^3, 1.74 kN/ m^3, 1.45 kN/m^3.

Based on the literature (Duan, H.G. et. al., 2011), the dosage of aggregate, cement, gypsum and water are all factors that affect the strength of the specimens. After many matching tests, a ratio that satisfies the requirement is selected (as shown in Table 2).

Table 2: The matching parameter table of rock mass similar material experiment for Luming north slope engineering.

Position	Lithology	Simulation of compressive Strength(MPa)	Simulated bulk density(kN/m^3)	The ratio of no.	Proportion material
1	Granite1	0.043	1.68	12:01:00	Sand, Lime, Gypsum
2	Granite2	0.102	1.728	873	Sand, Lime, Gypsum
3	Granite3	0.114	1.74	955	Sand, Lime, Gypsum
4	Crushed zone/ Fault	1.78×10^{-4}	1.45	-	Mica, Sand Mixture

4. THE FABRICATION OF SIMILAR MODEL AND ARRANGEMENT OF MEASURING POINTS

4.1 The fabrication of similar model

The building process of the similar model (Figure 2) of this project is as follows:

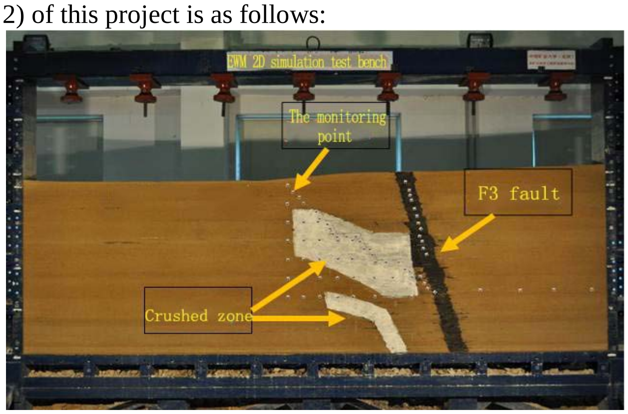

Figure 2: The similar mode of the west 3-3 profile for Luming Molybdenum.

Firstly set up the subject building of the model and compound the material, then smoothly place the material on the model. After the similar material is a little dry, remove the template and arrange the monitoring points.

4.2 Arrangement of the stress monitoring points

The strain gauges are arranged near the slope and crushedzone, in fault, at a total of 48, and the position of the specific placement is shown in Figure 3. As for the experiment limit, we mainly research the vertical strain. Pressure measurement applies to the testing system of the static strain, and the system includes a data collection box, a microcomputer and the supporting software.

4.3 The arrangement of the displacement monitoring points

In order to observe the slope surface and the regulation of the movement and deformations of overlying strata for the working face, the observation points of displacement are set up on the surface of the slope, the earth’s surface, and different positions of overburden layers for the molybdenum mine, respectively. The arrangement of designed points for a 3-3 profile similar model is shown in Figure 3.

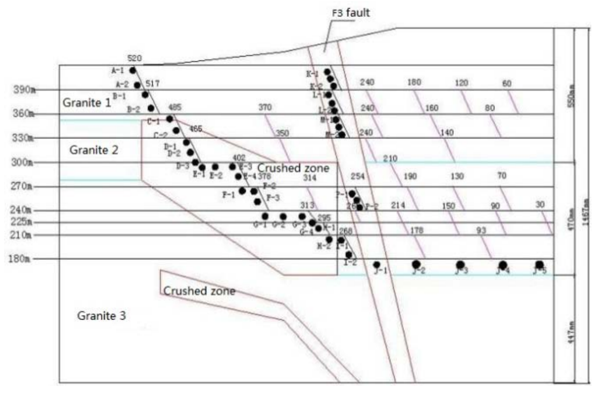

(a) General view of 3-3 section

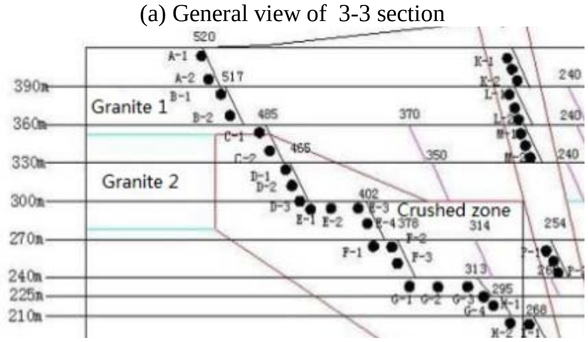

(b) Partial enlarged detail of 3-3 section
Figure 3: The arrangement of strain gauges, displacement monitoring points for 3-3 section similar model.

5. THE EXPERIMENT RESULTS OF SIMILAR SIMULATION ANALYSIS

The experiment results of 3-3 section stress change and displacement change were researched and analyzed, and eventually the section stability conditions were determined.

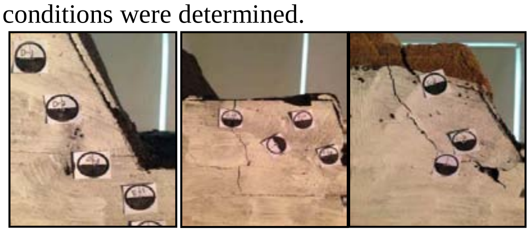

(a) Damage phenomenon of 360 m level

(b) Damage phenomenon of 330 m level

(c) Damage phenomenon of 300 m level

Figure 4: Deformation and damage of slope during excavation of 3-3 profile in the west area.

The analysis of Figure 4 shows that during the excavation of western 3-3 profile, 360 m, 330 m, 300 m represent elevation, and the macro deformation and failure of the slope are mainly embodied in the 360 m level, 330 m level and 300 m level. With the continuous excavation of the adjacent level, the original micro cracks penetrate mutually and expand continuously, resulting in obvious macro deformation and reduction.

5.1 Simulating analysis of stress variation about 3-3 section

The excavation is divided into 8 levels and the monitoring data of each excavation is acquired. Figure 5 is the stress monitoring data after each step of excavation.

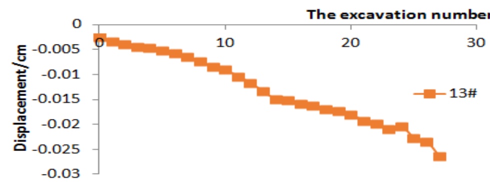

(a) 210 m level excavation stress change curve

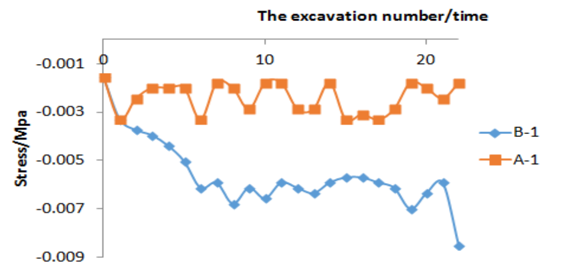

(b) 390 m and 360 m level excavation stress change curve

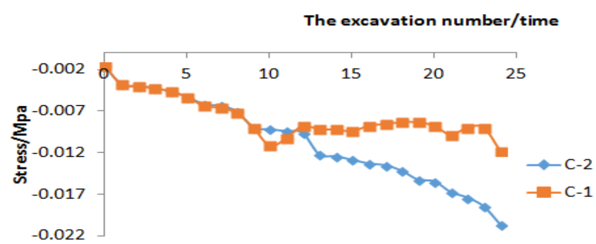

(c) 330 m level excavation stress change curve

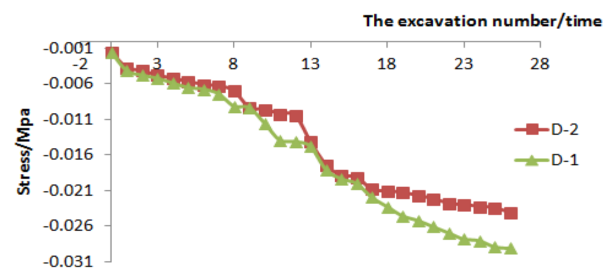

(d) 300 m level excavation stress change curve

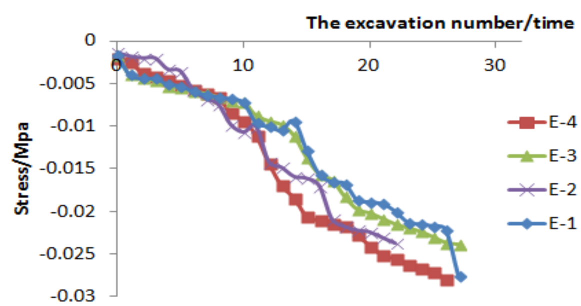

(e) 270 m level excavation stress change curve

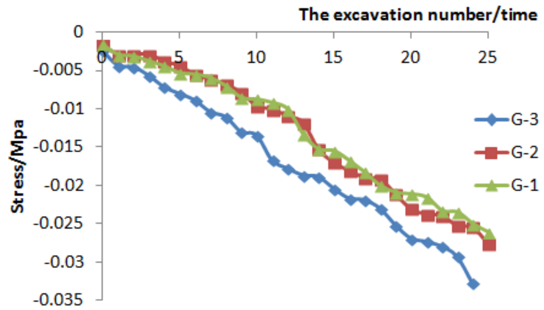

(f) 225 m level excavation stress change curve

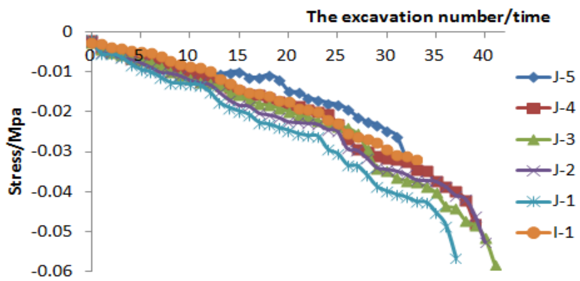

(g) 180 m level excavation stress change curve

Figure 5: The stress change curve of 3-3 profile during excavation in west area.

We can find from Figure 5 that:

(1) With the continuous excavation process, stress values from the 390 m-180 m level excavation had a rising stage, but overall the rise kept to a gentle degree.

(2) When excavation approached a certain level, its stress appeared to increase. After the exploiting was completed, stress reduced and pressure relieved quickly. Figure 5 shows that as for the NO.A-1 points (390 m level) and NO.B-1 points (360 m level), the two stress variation curves were parallel but the difference was relatively larger than other slopes, indicating that the stability of the 360 m level was poorer than other side slopes.

On the same level, stress change curves of two different monitoring points have large differences, indicating that the stability of the level is poor. The differences of the stress variation curve in the 330 m level and 300 m levels indicates that the stability was poorer than some other side slopes. There were some differences in stress curves in the 270 m, 225 m, 180 m levels nearby, indicating that there was a small possibility of slope instability during excavation. The 5# strain monitoring gauge at the 180 m level slope was laid in fault, and the rate of the stress changes was large, indicating there was the existence of instability phenomenon due to the fault through 180 m level slope.

In conclusion, 3-3 profile was not stable, the reason being that the slope was in the crushed zone, which resulted in instability phenomenon due to the variation of stresses.

5.2 The analog simulation displacement change rule of 3-3 profile

According to research data (Liu, L.P. et al.; 2000 Zeng, Y.W., 2005), in the slope stability analysis process, big displacement deformation of the slope occurs mainly in poor structural surfaces and bench slope areas. The similar simulation study focused on the 30 monitoring data analysis in the area near the bench slope and the monitoring results are shown in Figure 6.

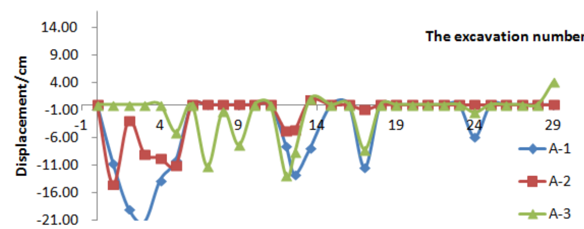

(a) The change curve of the 390 m level excavation displacement

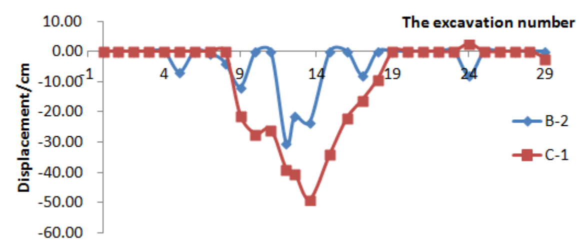

(b) The change curve of 360 m level excavation displacement

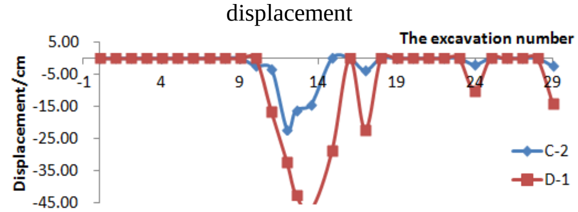

(c) The change curve of the 330 m level excavation displacement

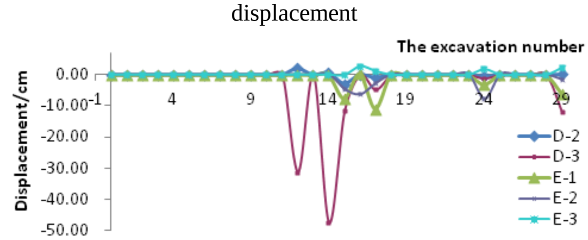

(d) The change curve of the 300 m level excavation displacement

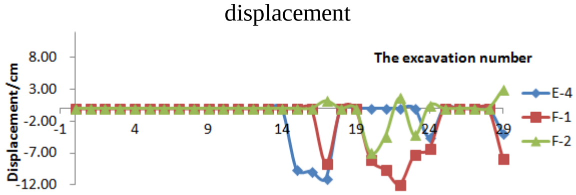

(e) The change curve of the 270 m level excavation displacement

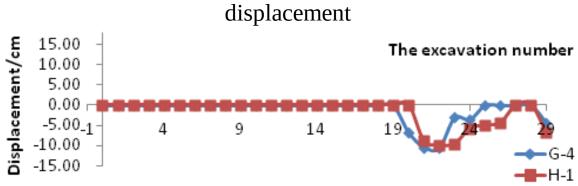

(f) The change curve of the 225 m level excavation displacement

Figure 6: 3-3 section displacement monitoring deformation.

As Figure 6 shows about the similar deformation and displacement monitoring figure of slope excavation, displacement has a certain change in the 29 times simulation of excavation process about the open pit slope. The negative displacement represents sink and positive displacement represents bounce. In Figure 6, from the displacement monitoring and deformation trend of excavation in the 180 m-390 m levels, we can find that the overall deformation of the slope is mainly in the sinking trend, with bounced as the secondary trend. The displacement of deformation ranges from a few centimeters to more than 20 centimeters. What we can analyze from the displacement deformation monitoring diagram and the picture of damaging during the excavating is that the fracture phenomena mainly appears in zone 360 m, zone 330 m, zone 300 m, and zone 270 m, which have F3 fault or are crossed by crushed zones. There is much more obvious fracture growing phenomena especially in the 300 m-360 m levels.

6. CONCLUSIONS

Based on the similar material simulation experiment, theoretical analysis of west-Ⅰarea Luming Molybdenum 3-3 section of the slope stability was analyzed, and the following conclusions were drawn:

In 3-3 section 360 m level, 330 m, 330 m level, the 180 m level stability are poorer, and instability may exist. The 3-3 section on 360 m level is the most likely to experience instability. To sum up, because the slopes are located in the fracture zone and the stress change leads to instability, the 3-3 profile is obviously not stable.

7. ACKNOWLEDGEMENT

It is with great pleasure that we acknowledge the generous financial support of National Natural Science Foundation of China (project number: 51474017) and Natural Science Foundation of Xinjiang Uygur Autonomous Region of China (2014211B013).

8. REFERENCES

Duan, H.G., Jiang, Z.Q., Zhu, S.Y., et, al.(2011). Centrifuge model tests on rock brusting induced by great depth highly stressed roof strata of weak structural plane. Journal of Central South University, Volume 31, NO. 9, pp: 2774-2782.

Liu, L.P., Jiang, D.Y., Zheng, S.C., et al. (2000). The recent progress of the slope stability analysis methods. Journal of Chongqing University(Natural Science Edition), Volume 15, NO.3, pp: 115-118.

Wu, W. (2011). The slope instability analysis of the causes and prevention and management. Mining Technology, Volume 12, NO. 5, pp: 44-46 .

Yang, T. H., Zhang, F. C., Yu, Q.L., et al. (2011). Research situation of open-pit mining high and steep slope stability and its developing trend. Rock and Soil Mechanics, Volume 32, NO.5, pp: 1437-1451, 1472.

Yin, Z.G, Li, X.F, Wei, Z.A, et al. (2011). Similar simulation study of deformation and failure. Chinese Journal of Rock Mechanics and Engineering, Volume 14, NO. 1, pp: 2913-2923.

Zeng, Y.W. (2005). Slope Stability Analysis By Combining Fem With Limit Equilibrium Method. Chinese Journal of Rock Mechanics and Engineering, Volume 7, NO. 2, pp: 5355-5359 .

Zhang, H., Liu, Q.S., Liao, X.G. (2011). Control and Support of Open - pit Slope. Mining Research and Development, Volume7, NO. 4, pp: 34-36, 40.